11PLF-0030

Effects of Washcoat on Initial PM Filtration Efficiency and Pressure Drop in SiC DPF

Author, co-author list (Do NOT enter this information. It will be pulled from participant tab in MyTechZone)

Affiliation (Do NOT enter this information. It will be pulled from participant tab in MyTechZone)

ABSTRACT

The washcoat (W/C) on a catalytic diesel particulate filter (DPF) greatly alters the pore structure and wall surface condition of the original substrate of DPF, which then affects the filtration efficiency and pressure drop behavior. In the present study, we examined this W/C effect on the initial PM filtration efficiency and pressure loss by changing amounts of washcoat on a SiC-DPF. We measured particle number concentration and particle size distribution in the diesel exhaust gas downstream of the DPF by EEPS. High filtration efficiency was achieved quickly when the W/C amount was increased. We introduced new parameters, T90 and T99, which were the filtration efficiencies that reach more than 90% and 99%, respectively, of the initial DPF usage. The PM trapping mechanisms could be classified according to the PM size. Trapping of PM whose diameter is smaller than 30 nm is little affected by the W/C. However, for PM over 30 nm, as amounts of W/C are increased, particle number concentration decreases rapidly and less PM leakage is observed for the initial filtration process. On the other hand, the initial backpressure and the backpressure during soot loading increased in accordance with W/C amount. Since the relationship between the filtration efficiency and the pressure loss has a trade-off, it is important to design DPF by considering W/C effects.

INTRODUCTION

Diesel engines have high thermal efficiency and good fuel economy, which represent an effective means of reducing CO_2 emissions when compared with equivalent gasoline engines. However, the soot (Particulate Matters, PM) contained in exhaust gas causes human health problems and environmental pollution, so that emission regulations for vehicles are becoming strict year after year. As one of the key technologies, a Diesel Particulate Filter (DPF) has been developed to reduce PM in the after-treatment of exhaust gas. The latest research has shown that the monolithic wall-flow DPF made of structured porous ceramic has very high filtration efficiency and can reduce PM by as much as 99% when a soot cake is formed [1 - 3]. On the other hand, the DPF needs to be periodically cleaned (regenerated) by burning the accumulated soot because the pressure loss increases as soot accumulates. The phenomenon of accumulation of very minute particles inside the DPF wall is difficult to visualize by experiments. Therefore, we have developed a numerical code to simulate the soot deposition and combustion processes in DPF [4 - 6].

Usually, the Pt catalyzed DPF for the soot oxidation at lower temperatures has a washcoat (W/C) layer consisting of alumina particles. Expectedly, this W/C greatly alters the original pore structure and wall surface condition of the substrate, which in turn affects the filtration efficiency and pressure drop behavior of DPF. Previous research has shown the effects of W/C and catalysis on characteristics of DPFs [2, 7 - 12]. In general, lower porosity and small pore size result in higher filtration efficiency [13]. However, the increase in the pressure loss becomes a concern because the permeability of the gas in the wall is worsened by the W/C.

It can be assumed that the nature of these changes will be determined by the material or physical properties of the filter substrate, and will also differ according to the differences in the W/C process. For example, the affinity of γ-alumina particles used for W/C differs for SiC and Cordierite. Differences in the structure of the wall with W/C may also possibly arise, according to porosity and pore size of non-W/C DPF. In addition, the mode of the change can be assumed to differ according to whether the γ-alumina particles of W/C uniformly cover the ceramic particle that composes the filter wall or whether the γ-alumina particles cause non-uniform blockage of

the narrow channels [14]. Therefore, if the nature of the structural changes of the filter wall caused by the W/C is understood, it is possible to optimize the W/C of DPF.

In the present study, the changes in the state of the filter wall structure induced by the W/C are discussed, based on changes in the pore distribution, and the influence on the performance of a SiC-DPF is examined. In particular, we examined the relationship between W/C amounts and initial PM filtration (that is, the short period of filtration efficiency seen at the initial DPF usage) and the pressure drop as soot loading occurs.

EXPERIMENT

TEST SAMPLES

A total of 5 wall-flow SiC-DPFs were prepared in this study. The specifications for these samples: size, Φ144mm× L 153mm; cell density, 300cpsi; wall thickness, 0.25mm. Sample A was a non-coated DPF, and the other samples were washcoated with different amounts of γ-alumina. Sample B had the typical base amount of W/C, while samples C, D, E had increasing amounts of W/C, at specific ratios to that of sample B. The pore structure characteristics were measured by mercury porosimetry (MICROMERITICS Co. AutoPore 9500) and a constant substrate specification of 16.5μm average pore size and 46.9% porosity (non-W/C :sample A) was used for all experiments. A summary of important parameters for the DPFs is given in Table 1. Figure 1 shows the surface structure of the filter wall as observed by SEM. Figure 1(a) is the non-W/C sample A, and Fig. 1(b) is the washcoated sample B. All samples (A～E) are non-catalytic filters.

Table 1 Sample specifications

Sample	A	B	C	D	E
Substrate	SiC				
Size (mm)	Φ144 × L153				
Cell Density (cpsi)	300				
Wall Thickness (mm)	0.25				
Porosity (%)	46.9	45.2	43.8	43.0	42.0
Median Pore Diameter (μm)	16.5	14.5	13.5	13.2	13.0
Washcoat	none	yes			
Coat amount / Coat amount $_B$	0	1	1.4	1.7	2.1
Pt Loading	none				

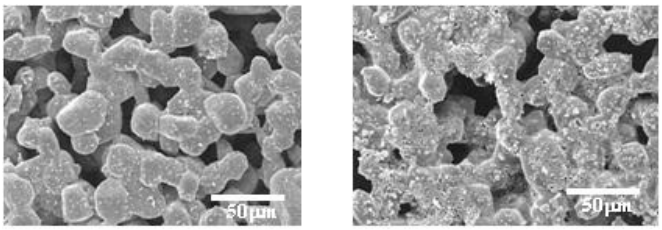

Figure 1 SEM image of (a) wall surface of uncoated DPF, (b) wall surface of W/C DPF

EXPERIMENTAL METHOD

The filtration efficiency of the DPF was evaluated with a QD32 Diesel engine (NISSAN) in this study. Table 2 shows the engine specifications. The engine was connected to an eddy current dynamometer (Tokyo Plant Co. ED-150) on the test-bench, with the test condition at 1400rpm and 190Nm load. A diesel oxidation catalyst (DOC; ACR Co. EXCAT C15) was used upstream of the DPF. To measure particle number concentration and particle size distribution in exhaust gas, an Engine Exhaust Particle Sizer (TSI Co. EEPS 3090) was used in conjunction with a flow path selection system to provide samples downstream of the DPF. A schematic of the experimental setup is shown in Fig. 2. The sampling gas was diluted by 350℃ air to remove volatile matters. Hence, all EEPS measurements referred to solid soot aggregates. For the case without a DPF, a flange with orifices was used instead of a DPF downstream of the EEPS conjunction point for equivalent backpressure of DPF.

Table 2 Engine specifications

Model	NISSAN QD32 OHV diesel
Type	4 stroke
Cylinders	4, in-line
Valve mechanism	swirl chamber
Displacement	3.153L
Rated Power	72 kW @3600 rpm
Peak Torque	216 Nm @2000 rpm
EGR System	none
Turbocharger	none (NA)

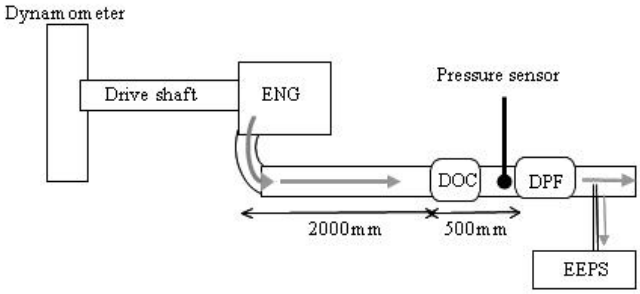

Figure 2 Experimental setup

As shown in Fig. 2, the pressure drop was measured as backpressure with a pressure sensor (KEYENCE Co. AP-32A) in front of the DPF. The soot load amount was calculated by the weight increase of the DPF every 15 minutes.

RESULTS AND DISCUSSION

ANALYSYS OF PORE STRUCTURE

Figure 3 shows the variations of the porosity and the average pore size with W/C amount. As the W/C amount increases, the porosity and the average pore size decrease. The pore distribution was measured to investigate the alteration of the structure by the W/C. Figure 4 shows the pore size distribution for samples A, C, and E. Compared to non-W/C sample A, the peaks of pore distribution of samples C and E (washcoated samples) shift to smaller pore sizes of around 10μm. As the amount of W/C increases, the volume of minute pore sizes increases. That is, a huge number of pores increase with W/C, because the pore volume of the minute pore size increases.

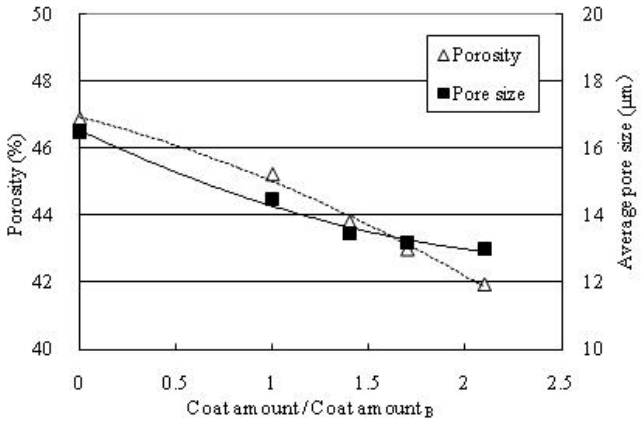

Figure 3 Variations of porosity and average pore size with W/C amount

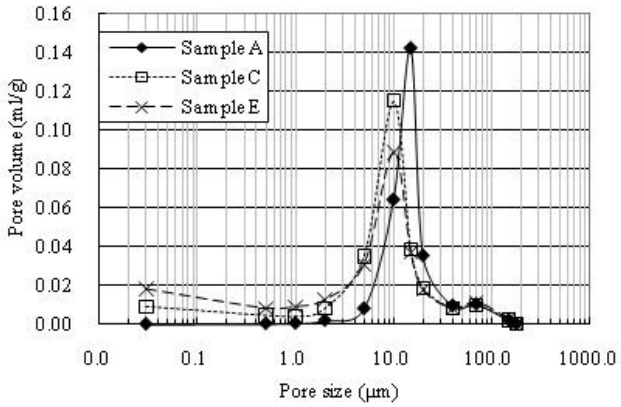

Figure 4 Pore size distribution

Next, the relationship between the surface area per unit mass of the filter wall and W/C amount was investigated, as was the relationship between the pore volume under 0.5μm and the W/C amount. These results are shown in Fig. 5. As the amount of W/C increases, the surface area increases, especially when the ratio of W/C amount is over 1.5. In the case of sample E, the surface area is ten times larger than that of non-W/C DPF. The increase in surface area also corresponds with the increase in pore volume under 0.5μm.

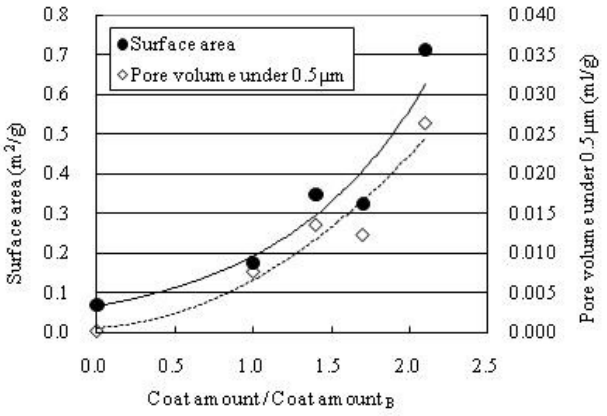

Figure 5 Relationship between W/C amount and surface area per unit mass of the filter wall, pore volume under 0.5μm

In general, the W/C material in a DPF consists of γ-alumina particles with a diameter range from 0.1 to 1.0 μm, and these particles are porous materials that have nanopores [12, 15]. Figure 6 shows the structure of γ-alumina particles observed by SEM. When these minute particles adhere to the SiC grains that compose the filter wall, the porosity and the pore size expectedly decrease. As seen in Fig. 4, it should be noted that the peak positions in pore distribution of samples C and E are the same (as are samples B and D), but the pore volume of the peak is decreased in comparison with non-W/C DPF of sample A, suggesting that the pores made of gaps in the SiC grains become narrowed or blocked by γ-alumina particles. However, the number of channels blocked with γ-alumina particles increases as the W/C amount increases.

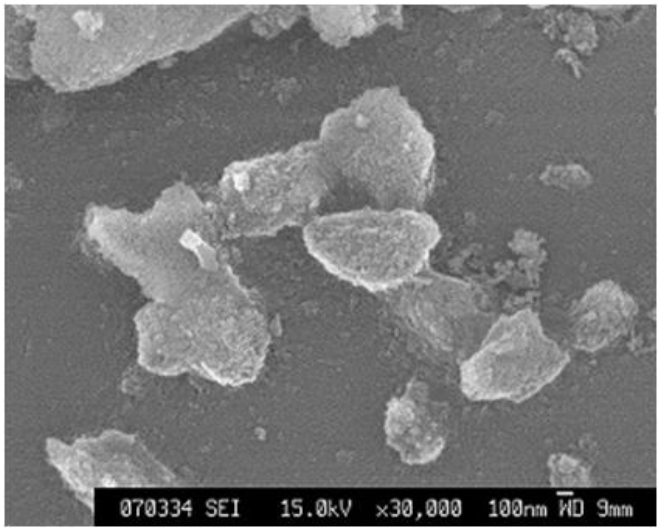

Figure 6 SEM image of γ-alumina particles

These results regarding mercury porosimetry show that not only are the porosity and the pore size altered by the W/C, but also is the structure of filter wall. In the following section, we investigated the effects of W/C on characteristics of DPF.

FILTRATION EFFICIENCY

Figure 7 shows the number-based filtration efficiency upon initial usage for DPF samples A, C, and E. The filtration efficiency was measured by the EEPS and calculated as:

$$Filtration\ \ efficiency\ = \left(1-\frac{N_1}{N_0}\right)\times 100 \qquad (1)$$

where N_0 is the total particle number concentration in case without the DPF, and N_1 is the total particle number concentration downstream of each DPF. It is found that the filtration efficiencies for samples C and E (washcoated samples) are about 100% at 60 s, while in the case of sample A (non-W/C), the filtration efficiency has yet not reached 100% by 120 s. Therefore, the filtration efficiency quickly becomes high in accordance with the increase in the W/C amount. It is well-known that the high filtration efficiency is achieved once the soot layer (cake) is formed on the DPF wall [1 - 3]. Accordingly, it is considered that the soot cake appears quickly in the case of a washcoated DPF.

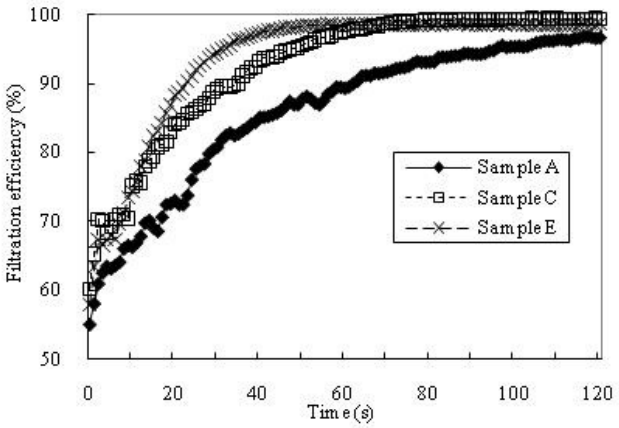

Figure 7 Number-based filtration efficiency upon initial usage for DPF samples A, C, and E

Next, the time-variation of filtration efficiency was examined. Here, we introduced new parameters: T90 and T99; where T90 is the time to reach more than 90% filtration efficiency, and T99 is the time to reach more than 99% filtration efficiency, from initial filtration usage. For example, Fig. 8 shows T90 and T99 obtained for the initial PM filtration efficiency with sample C. Figure 9 shows the relationship between the W/C amount and T90 and T99. In accordance with the increase in the W/C amount, T90 and T99 can be shortened. In particular, in the case where the W/C amount ratio is around 2.0, T99 is only one third of the non-W/C value. If the filtration efficiency quickly reaches a high value, it would appear that the PM breakthrough to the atmosphere through a DPF could be reduced in the early filtration times. In other words, in order to achieve high filtration efficiency of more than 99% quickly, it seems that the W/C on a DPF is needed.

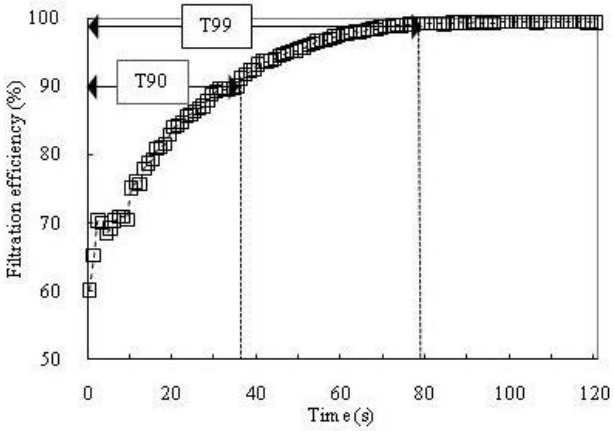

Figure 8 Time-variation of filtration efficiency with parameters of T90 and T99; T90 is the time to reach more than 90% filtration efficiency, and T99 is the time to reach more than 99% filtration efficiency, from initial filtration usage

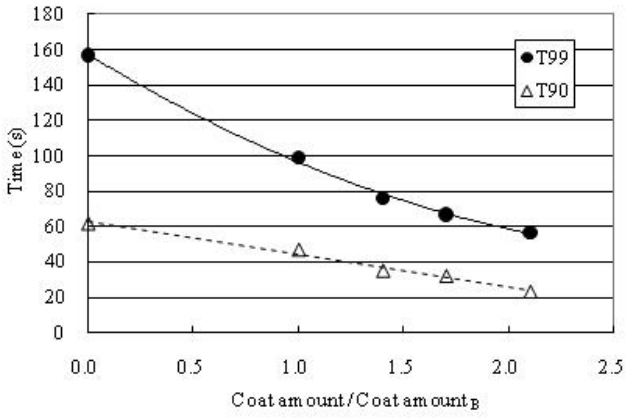

Figure 9 Relationship between W/C amount and T90 and T99

We then compared the particle size distribution downstream of each DPF. The changes in PM size distribution downstream of samples A, C, and E are shown in Fig. 10. The particle size distribution in the exhaust gas has a peak around 80nm, and the particle concentration is about 10^7 1/cm^3 without a DPF. Also, it is found that the diameter of particles is mainly from 30nm to 200nm. As seen in this figure, the leakage of over 100 or 200nm PM for samples C and E (washcoated samples) is reduced compared with sample A (non-W/C sample) on initial PM filtration (0 s) [16]. The particle number concentrations of leakage for samples C and E are lower than that of sample A at 20 s after the initial PM filtration. At time = 120 s, although the PM leakage around 80nm for sample A is still observed, all sizes of PM for samples C and E are very close to the lower detection limit of the EEPS.

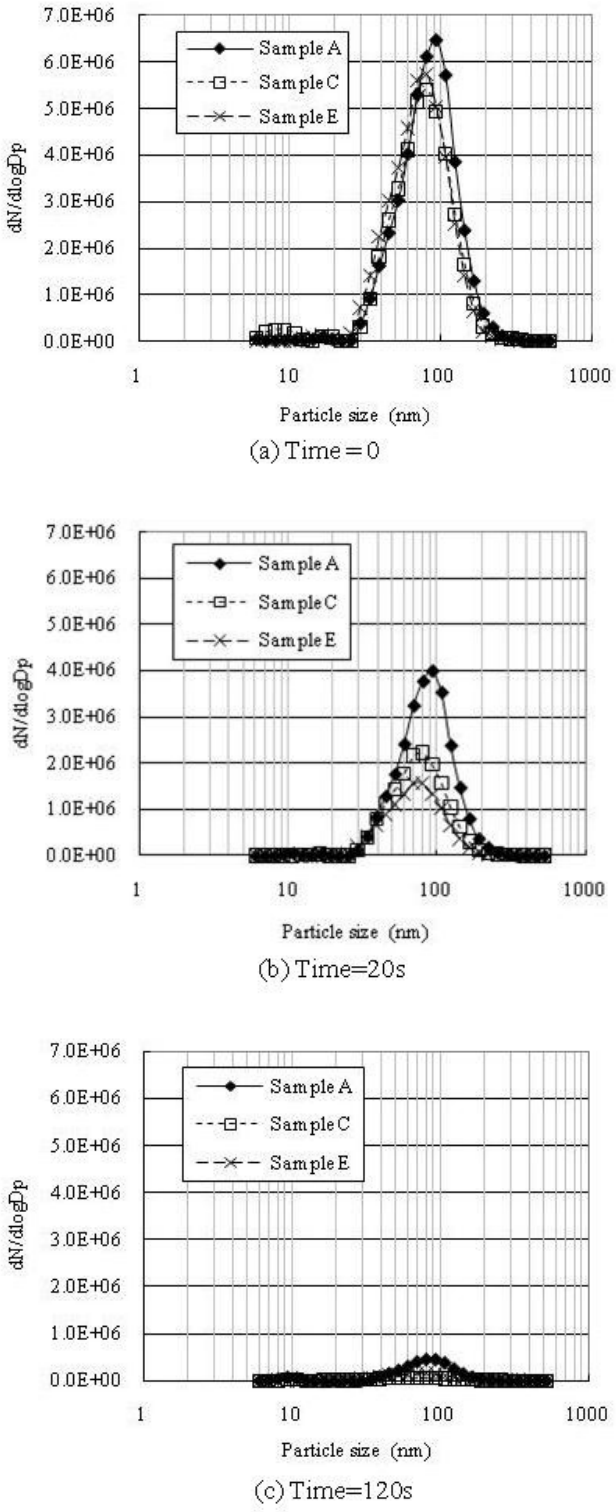

Figure 10 Particle size distributions downstream of samples A, C, and E

It has been reported that the coefficient of determination of the PM trapping mechanism in a DPF depends on PM size [17]. According to Hayashi and Kubo [18], it has been reported that particles less than 300nm is trapped by "the Brownian diffusion" whereas particles over 300nm are trapped by "the direct interception". However, as above mentioned, the particle size distribution has a peak around 80nm, and most of the particle number concentration is composed from 30nm to 200nm, which contributes greatly to the soot layer

formation for high filtration efficiency. Then, we examined the effect of W/C on PM filtration by considering three PM size groups in the range of under 30nm, 30～200nm, or over 200nm.

Group 1 consists of the very minute PM under 30nm which is mainly trapped by Brownian diffusion. As shown in Fig. 10, the particle number concentrations of trapped PM under 30nm are almost same for all samples of W/C or non-W/C DPFs. Based on this result, altering the filter wall structure by W/C appears to have no influence on PM adsorption by Brownian diffusion (see Fig. 11(a)). This is because the PM size (under 30nm) is much smaller than the γ-alumina particles coated on the filter wall.

Group 2 consists of 30～200nm PM. This group is considered to have the greatest particle number concentration and contributes greatly to the soot layer formation for high filtration efficiency. Since the average pore size is decreased by W/C in Fig. 3, the channel is easily blocked by PM to form a soot layer, so that the filtration efficiency can reach a high value in a short time (Figs. 7, 9, 11(b)). As seen in Fig. 4, due to excessive W/C amounts, the increase in blocked channels by γ-alumina particles cause blockage of the remaining left channels, and the soot layer forms even more quickly.

Group 3 consists of larger particles, PM over 200nm, compared to groups 1 and 2. As shown in Fig. 10, PM over 200nm is trapped more efficiently at the start of filtration, suggesting that the larger PM is more affected by W/C. Since a large PM has relatively large mass, it has a substantial inertia compared to the small PM in groups 1 and 2. Therefore, since the motion of PM over 200nm is likely to be in a beeline, the trapping mechanism is greatly affected by "interception" and "inertial impaction". An uneven surface of ceramic grains caused by W/C can result in easy trapping of this large PM at the initial filtration without a soot layer (Fig. 11(c)).

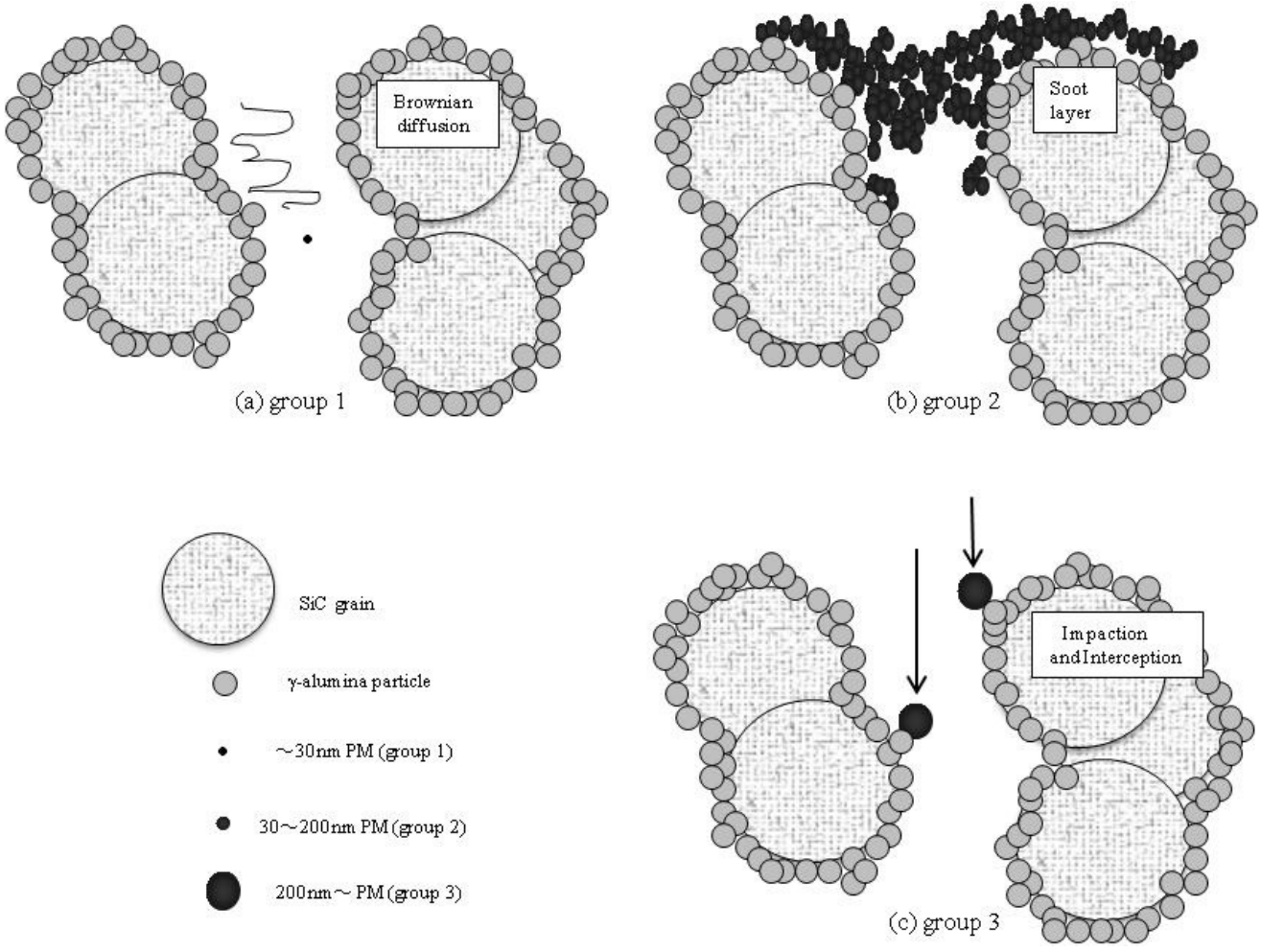

Figure 11 Particle trap mechanism classified according to PM size

the case of minute PM, trapping is mainly by "Brownian diffusion", and the larger PM is more effectively trapped by "interception" and "inertial impaction".

PRESSURE LOSS

It is expected that increase in pressure loss caused by the decrease of gas permeability is enhanced when the porosity and the average pore size are decreased by W/C [19]. We investigated the relationship between W/C amount and the initial backpressure (no PM loading) in Fig. 12. Here, the initial backpressure measurement was carried out under the cold flow condition, and the air flow rate at room temperature was 4Nm^3/min. The initial backpressure becomes high, the increase in the W/C amount; in particular, when the ratio of W/C amount is more than around 1.5.

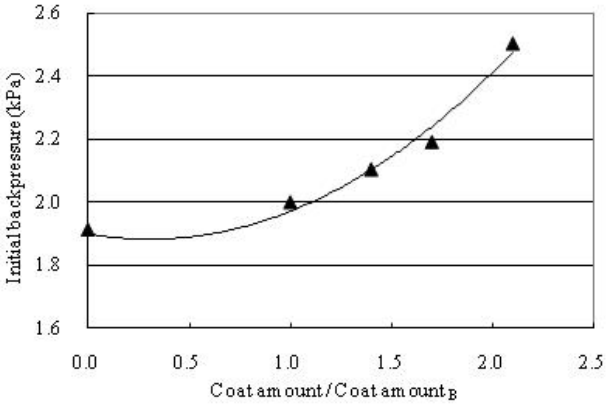

Figure 12 Relationship between W/C amount and initial backpressure (no PM loading)

Figure 13 shows the backpressure during soot loading for all samples. The backpressure increases almost linearly during soot loading, and increases as W/C amount is increased. Figure 14 shows the increasing rate (the slope of the backpressure in Fig. 13) during soot loading for samples A, C, and E. The increasing rate becomes larger as W/C amount is increased. The backpressure increases with soot loading because the thickness of the soot cake increases once the soot layer is initially formed on the surface of the filter wall. Here, the total pressure loss, ΔP, due to soot loading can be expressed as:

$$\Delta P = \Delta P_0 + \Delta P_1 \qquad (2)$$

where ΔP_0 is the initial pressure loss across the filter wall, and ΔP_1 is the pressure loss caused by the soot cake [20]. The image of ΔP is shown in Fig.15. Expectedly, ΔP_1 is almost equal for each sample when there is the same amount of soot loading [21]. However, the increasing rate is larger in accordance with an increase in the W/C amount (Figs. 13 and 14). Accordingly, ΔP_0 across the filter wall is considered to increase slightly during soot loading after soot layer formation. Therefore, it is considered that the PM breaks through the soot cake and reaches the inside of the filter wall. This PM then blocks the narrow channel and makes a new bridge, especially for the filter wall with the W/C.

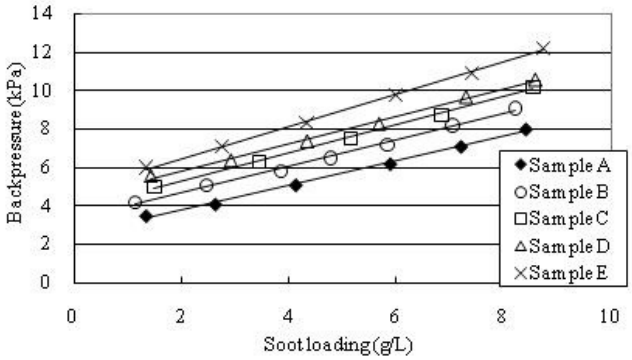

Figure 13 Backpressure during soot loading for all samples

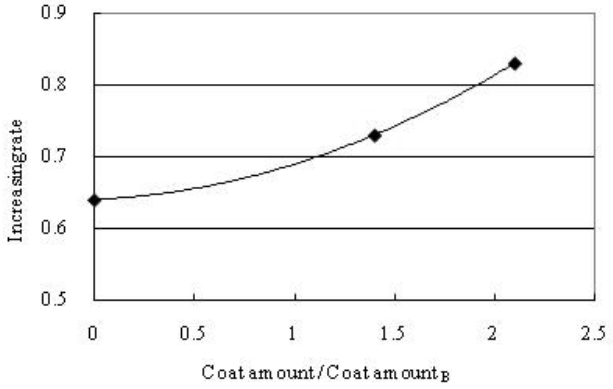

Figure 14 Increasing rate, which is the slope of the backpressure in Fig. 13, during soot loading for samples A, C, and E

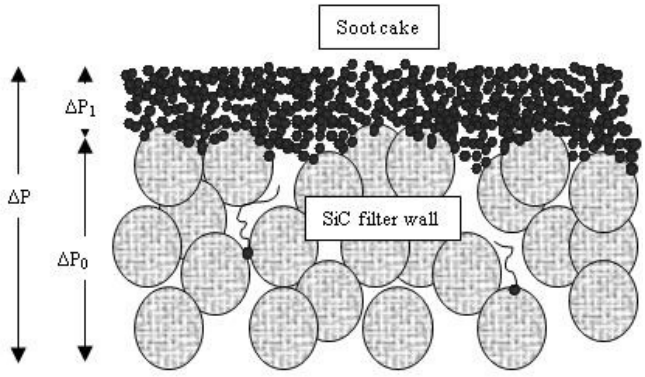

Figure 15 Image of total pressure loss during soot loading; ΔP is total pressure loss, ΔP_0 is initial pressure loss across filter wall, and ΔP_1 is pressure loss caused by soot cake

Based on the above-mentioned results, both the initial backpressure and the backpressure during soot loading increase in accordance with increases in the W/C amount. Figure 16 shows the relationship between the backpressure of 8g/L soot loading and the W/C amount. It may be noted that a value of 8g/L is one of the standard soot load amounts for regeneration. In Fig. 16, for a ratio of W/C amount of 1.0, a backpressure of 8g/L soot loading is about 15% higher than a non-W/C sample; however, for a ratio of W/C amount of 2.0, the backpressure of 8g/L soot loading is about 50% higher than a non-W/C sample. This means that the backpressure of soot loading increases rapidly with excess amounts of W/C.

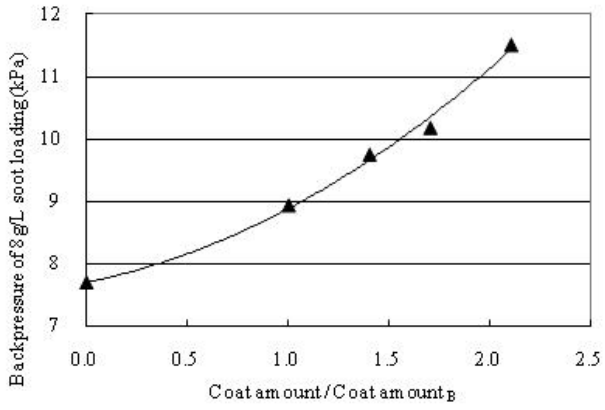

Figure 16 Relationship between backpressure of 8g/L soot loading and W/C amount

EFFECT OF W/C ON INITIAL PM FILTRATOIN EFFICIENCY AND PRESSURE LOSS

High filtration efficiency is expected in relation to increases in W/C amount, especially with respect to the large reduction of PM leakage for initial DPF usage. However, the initial backpressure and the backpressure during soot loading will increase in accordance with the W/C amount. It should be noted that some W/C amount is needed in the process of catalyst coating. A diagram of the relationship between the W/C amount and pressure loss, initial PM filtration efficiency is shown in Fig. 17. It shows that the proper W/C amount exists, which has high filtration efficiency with relatively low pressure loss. Conversely, in the case of excessive W/C amount, although filtration efficiency will be as high as with the proper amount of W/C, the pressure loss will increase greatly. Therefore, it is important to determine W/C amount with high filtration efficiency and low pressure loss for appropriate design of DPF.

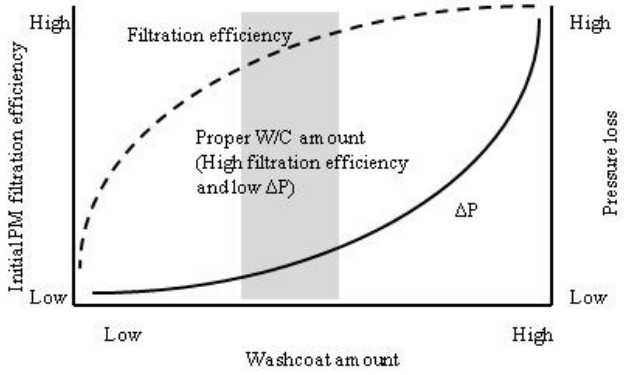

Figure 17 Diagram of relationship between W/C amount and pressure loss, initial PM filtration efficiency

CONCLUSIONS

We examined the effects of W/C on the initial PM filtration efficiency and pressure loss in a DPF with different amounts of W/C. The following results were derived.

(1) Both the porosity and the pore size as well as the structure of the filter wall are altered by adhering γ-alumina particles to SiC grains composing the filter wall to increase the volume of minute nanopores. Consequently, the channel becomes narrower and the number of blocked channels increases along with increases in the amount of W/C.

(2) The filtration efficiency becomes high after formation of the soot cake. The time to reach more than 90% filtration efficiency (T90) and more than 99% filtration efficiency (T99) from initial filtration usage can be shortened as the W/C amount increases.

(3) The initial backpressure and the backpressure during soot loading increase in response to the W/C amount. Since the relationship between the filtration efficiency and the pressure loss has a trade-off, it is important to design DPF by considering W/C effects. There is the proper W/C amount with high filtration efficiency and relatively low pressure loss.

REFERENCES

1. Wirojsakunchai, E., Schroeder, E., Kolodziej, C., Foster, E. D., Schmidt, N., Root, T., Kawai, T., Suga, T., Nevius, T., and Kusaka, T., "Detailed Diesel Exhaust Particulate Characterization and Real-Time DPF Filtration Efficiency Measurements During PM Filling Process," SAE Technical Paper 2007-01-0320.
2. Karin, P., Cui, L., Rubio, P., Tsuruta, T., and Hanamura, K., "Microscopic Visualization of PM Trapping and Regeneration in Micro-Structural Pores of a DPF Wall," SAE Technical Paper 2009-01-1476.
3. Tsuneyoshi, K., Takagi, O., Yamamoto, K., "Effect of Surface Roughness on Initial PM Filtration Efficiency of DPF," *Transactions of the Japan Society of Mechanical Engineers*, Series B, Vol.76, No.767:100-107, 2010.
4. Yamamoto, K., Oohori, S., Yamashita, H., Daido, S., "Simulation on Soot Deposition and Combustion in Diesel Particulate Filter," *Proceedings of the Combustion Institute, Volume 32*, The Combustion Institute:1965-1972, 2009.
5. Yamamoto, K., Satake, S., Yamashita, H., "Microstructure and Particle-laden Flow in Diesel Particulate Filter, " *Int. J. Thermal Sciences*, Vol.48:303-307, 2009.
6. Yamamoto, K., Nakamura, M., Yane, H., and Yamashita, H., "Simulation on Catalytic Reaction in Diesel Particulate Filter," *Catalysis Today*, Vol.153:118-124, 2010.
7. Merkel, A. G., Cutler, A. W., Tao, T., Chiffey, A., Phillips, P., Twigg, V. M., and Walker, A., "New Cordierite Diesel Particulate Filters for Catalyzed and Non-Catalyzed Applications," presented at 9th Diesel Engine Emissions Reduction Conference, 2003.
8. Kuwajima, M., Okawara, S., Tsuzuki, M., Yamaguchi, M and Mastuo, S., "Analysis of Sophisticated DPNR Catalyst, Focused on PM Particle Number Emissions," SAE Technical Paper 2009-01-0290.
9. Daido, S., Takagi, N., "Visualization of the PM Deposition and Oxidation Behavior Inside the DPF Wall," SAE Technical Paper 2009-01-1473.
10. Lorentzou, S., Pagkoura, C., Konstandopoulos, G. A., and Boettcher, J., "Advanced Catalyst Coating for Diesel Particulate Filters," SAE Technical Paper 2008-01-0483.
11. Ogyu, K., Oya, T., Ohno, K and Konstandopolous, G. A., "Improving of the Filtration and Regeneration Performance by the SiC-DPF with the Layer Coating of PM Oxidation Catalyst," SAE Technical Paper 2008-01-0621.
12. Ohyama, N., Nakanishi, T., and Daido, S., "New Concept Catalyzed DPF for Estimating Soot Loadings from Pressure Drop," SAE Technical Paper 2008-01-0620.
13. Fukushima, S., Ohno, K., Vlachos, N., and Konstandopoulos, A. G., "New Approach for Pore Structure and Filtration Efficiency Characterization," SAE Technical Paper 2007-01-1918.
14. Mey, D., Andy, P., Tardivat, C., Augier, C., and Briot, A., "Improved DPF Substrate for Washcoat Accommodation," SAE Technical Paper 2009-01-0288.
15. Stary, T., Solcova, O., Schneider, P., and Marek, M., "Effective diffusivities and pore-transport characteristics of washcoated ceramic monolith for automotive catalytic converter," *Chemical Engineering Science*, Volume 61:5934-5943, 2006.
16. Zarvalis, D., Lorentzou, S., and Konstandopoulos, G. A., "A Methodology for the Fast Evaluation of the Effect of Ash Aging on Diesel Particulate Filter Performance," SAE Technical Paper 2009-01-0630.
17. Ohara, E., Mizuno, Y., Miyairi, T., Mizutani, T., Yuuki, K., Noguchi, Y., Hiramatsu, T., Makino, M., Takahashi, A., Sakai, H., Tanaka, M., Martin, A., Fujii, S., Busch, P., Toyoshima, T., Ito, T., Lappas, I., Vogt, C. D., "Filtration Behavior of Diesel Particulate Filters (1)," SAE Technical Paper 2007-01-0921.
18. Hayashi, H., Kubo, S., "Computer simulation study on filtration of soot particles in diesel particulate filter," *Computers & Mathematics*, Application 55:1450-1460, 2008.

19. Zuberi, B., Liu, J. J., Pillai, C. S., Weinstein, G. J., Konstandopoulos, G. A., Lorentzou, S., and Pagoura, C.,“Advanced High Porosity Ceramic Honeycomb Wall Flow Filters,”SAE Technical Paper 2008-01-0623.
20. Tanaka, N., Ohno, K., Hong, S., Sato, H., Yoshida, Y., and Komori, T.,“Effect of SiC-DPF with High Cell Density for Pressure Loss and Regeneration,”SAE Technical Paper 2001-01-0191.
21. Rose, D., Boger, T.,“Different Approaches to Soot Estimation as Key Requirement for DPF Applications,”SAE Technical Paper 2009-01-1262.

CONTACT INFORMATION

R&D Center TYK Corporation
3-1 Ohbata-cho, Tajimi-City, Gifu Pref, 507-8607 Japan
E-mail:ku.tsuneyoshi@tyk.jp